Scattering of 31.5-Mev Positive Pions from Carbon

P. P. KANE*
Department of Physics, University of Rochester, Rochester, New York
(Received July 10, 1958)

Measurements were made at laboratory angles from 40° to 145° on the scattering of 31.5-Mev positive pions from carbon. Pulse-height analysis was used to select elastic scattering events. The observed differential cross sections for elastic scattering indicate destructive interference between the Coulomb and nuclear scattering amplitudes. The presence of inelastic pion scattering is inferred from a combination of different methods of study: pulse-height analyses, absorption measurements, and detailed comparisons of the data obtained in the case of carbon with those obtained in the case of copper and lead. An upper limit of 2 is placed on the spin of the 9.6-Mev state of C^{12}. This is not in disagreement with the results of other experiments and existing theoretical predictions.

1. INTRODUCTION

THE scattering of low-energy pions from carbon has been studied in many laboratories. In addition to the early measurements made at Cornell,[1,2] there exist the Columbia experiments[3,4] at 62 Mev and at 80 Mev. Although inelastic scattering of pions leading to large energy losses was observed by Byfield *et al.*, the 80-Mev experiment was the first to exhibit pion scattering involving excitation of low-lying states of carbon. As a by-product of the pion-nucleon scattering investigation program, data were obtained at Rochester[5] on the angular distribution of elastic scattering of 40-Mev positive pions from carbon. In order to increase the relative effectiveness of the S-state pion-nucleon scattering amplitudes, we decided to make measurements on the nuclear scattering of pions at an energy below 40 Mev. The theoretical treatment[6–15] of the problem emphasizes the great importance of a clear separation of elastic scattering from other processes. For an adequate understanding of the experimental results, such a separation is necessary. In Baker's experiment[4] the separation was made by a differential range technique. In the present experiment, substantial attention was again devoted to the question of a good criterion for the selection of purely elastic scattering events. However, the adopted procedure was different. It is described in Sec. 3. Since the energy difference between the ground state and the first excited state of C^{12} is about 4.4 Mev[16] and since the higher excited states are also rather well separated in energy, this element was the obvious choice as the scatterer. Even with this choice, it was essential to have a pion beam of well-defined energy. Such beams were not available at energies lower than about 30 Mev. Hence the experiments were performed in the 30-Mev range.

2. EXPERIMENTAL ARRANGEMENT

The positive pion beam was obtained by bombarding an aluminum target in the Rochester synchrocyclotron and using the focusing properties of the fringing magnetic field. Additional energy selection was provided by a magnet with sector-shaped pole pieces. In order to reduce the lateral blow-up of the beam resulting from multiple Coulomb scattering in air, helium paths were used over a considerable length of the beam trajectory. The general arrangement is shown in Fig. 1. A typical range curve of the incident beam shows that there is an 8.5% contamination of the beam, mostly attributable to muons and electrons.

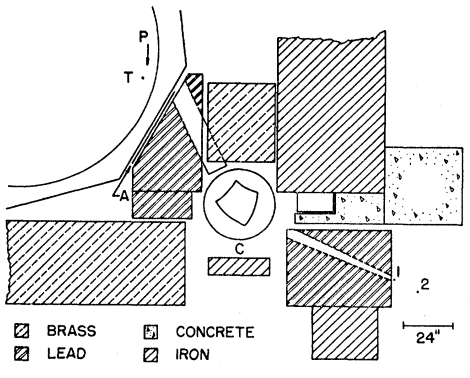

FIG. 1. Pion beam arrangement at the cyclotron. Arrow near P indicates the proton beam. T specifies target location. A is an absorber which is useful in reducing the energy spread of the pion beam. C stands for the analyzing magnet. Two counters 1 and 2 define the incident beam.

* Present address: Wesleyan University, Middletown, Connecticut.
[1] M. Camac *et al.*, Phys. Rev. **82**, 745 (1951).
[2] A. M. Shapiro, Phys. Rev. **84**, 1063 (1951).
[3] Byfield, Kessler, and Lederman, Phys. Rev. **86**, 17 (1952).
[4] W. F. Baker, Nevis Cyclotron Report 48 (unpublished).
[5] J. Perry, Doctoral dissertation submitted to the University of Rochester, 1953 (unpublished).
[6] Isacs, Sachs, and Steinberger, Phys. Rev. **85**, 718 (1952).
[7] H. A. Bethe and R. R. Wilson, Phys. Rev. **83**, 690 (1951).
[8] D. C. Peaslee, Phys. Rev. **87**, 863 (1952).
[9] W. W. Wada, Phys. Rev. **92**, 152 (1953).
[10] D. H. Stork, Phys. Rev. **93**, 868 (1954).
[11] L. S. Kisslinger, Phys. Rev. **98**, 761 (1955).
[12] Pevsner, Rainwater, Williams, and Lindenbaum, Phys. Rev. **100**, 1419 (1955).
[13] A. Pevsner and J. Rainwater, Phys. Rev. **100**, 143 (1955).
[14] Williams, Baker, and Rainwater, Phys. Rev. **104**, 1695 (1956).
[15] Frank, Gammel, and Watson, Phys. Rev. **101**, 891 (1956).
[16] F. Ajzenberg and T. Lauritsen, Revs. Modern Phys. **27**, 77 (1955).

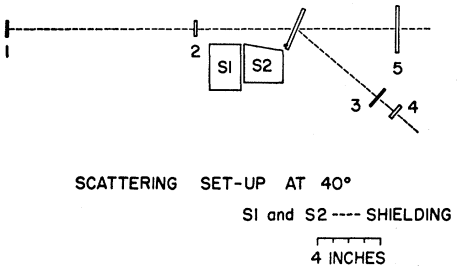

FIG. 2. Scattering set-up for 40° measurements.

The incident beam was defined by two counters, called 1 and 2. Two counters, 3 and 4, defined the scattered beam. The 1–2–3–4 accidental counting rate was not large. However, an anticoincidence counter, labelled 5, was used to make it negligible. All scintillators were made of the Sintilon type of plastic phosphor. Counters 1, 2, and 3 were mounted on RCA-1P21 photomultiplier tubes, the fourth on RCA-6655, and the fifth on RCA-6810. All counters, except the fourth, were one-eighth inch in thickness. The fourth was one-quarter inch thick. The first two counters were 1 in. $\times$2 in., the third was $1\frac{1}{2}$ in.$\times$4 in., the fourth was 1 in.$\times$4 in. and the fifth was 3 in.$\times$4 in. The fourth counter defined the solid angle subtended at the target. The arrangement of the counters in a typical scattering measurement is shown in Fig. 2.

The pulses from all counters were sent to broad-band amplifiers and then to fast-diode-coincidence circuits. The output of each coincidence circuit was in turn amplified and fed to a trigger generator, employing an EFP60 tube and delivering pulses of length 0.09 microsecond. In order to achieve good time resolution, 1–2 and 1–3–4 coincidences were made in the cyclotron room itself. A typical delay curve revealed resolving times of the order of 20 millimicroseconds with a flat-top region of at least 10 millimicroseconds. In the research room, the 1–2 trigger generator output and the fifth counter output were used to give pulses corresponding to 1–2–5 and 1–2–$\bar{5}$ events. The 1–2–$\bar{5}$ pulse was in turn combined with the 1–3–4 trigger generator output to give pulses corresponding to 1–2–3–4–$\bar{5}$ events. Such events represent interactions between the incident beam and the target. The efficiency of the 1–3–4 coincidence circuit was measured to be 96.7$\pm$2%.

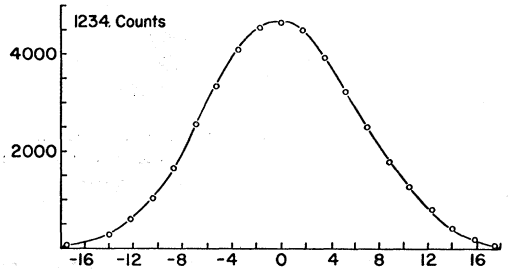

FIG. 3. Angular spread of the beam about the forward direction.

The total angular spread of the beam about the forward direction, resulting from the initial beam spread, multiple Coulomb scattering in the target, and pion decay, was measured by rotating the scattering counters 3 and 4 about the zero-degree position. The resulting curve is shown in Fig. 3. The width of the curve at half height is $\pm$7 degrees and is a measure of the angular acceptance of the scattering counters.

The pulses from the tenth dynode of the fourth counter were fed to a cathode follower, the output of which was used for pulse-height analysis. Pulse-height measurements were made at the laboratory angles 40°, 55°, 70°, 90°, 105°, 120°, and 145°. The background was determined from the pulse-height spectrum obtained in the absence of the carbon target. During the background measurements, an absorber was placed between counters 3 and 4 to provide the same degradation of energy as that resulting from the carbon target. At 40°, the background was about one-fifth of the counting rate due to elastic pion scattering from carbon. It was much smaller at larger angles.

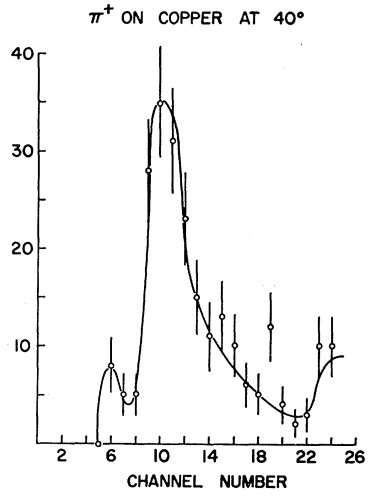

FIG. 4. Pulse-height spectrum of scattered beam for copper at 40°. The scintillator used for pulse-height analysis was $\frac{1}{4}$ in. thick. Lower energy pions appear in higher pulse-height channels and vice versa. The peak around channel 10 corresponds to elastically scattered pions. Counts in the neighborhood of channel 6 represent positrons and positive muons.

3. SCATTERED BEAM COMPOSITION

The "scattered" beam actually contains positrons, muons, protons, and both elastically and inelastically scattered pions. Whenever the intensity of the competitive components is large, it is difficult to determine accurately the number of elastically scattered pions. Therefore, a reliable method for extracting the elastic pion scattering contribution had to be developed. The method depended upon the calibration of the pulse-height-analyzing part of the electronics by means of the incident beam. The target was oriented so as to minimize the energy spread of the scattered beam (Fig. 2). With such a target orientation, the mean target thickness traversed by the beam during calibrations was the same as that traversed during scattering measurements. Therefore, knowing the shape of the

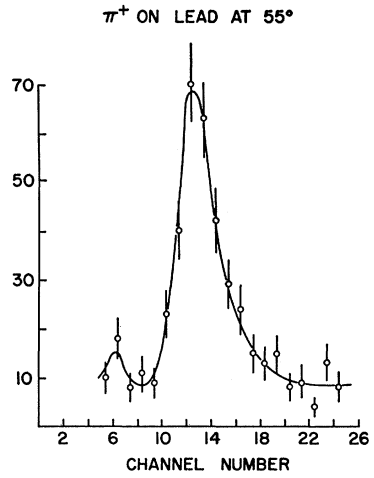

FIG. 5. Pulse-height spectrum for lead at 55°. The peak around channel 13 corresponds to elastically scattered pions. Counts in the neighborhood of channel 6 represent positrons and positive muons.

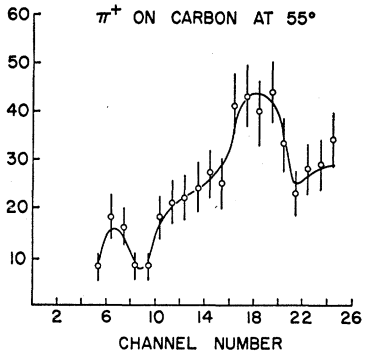

FIG. 7. Pulse-height spectrum for carbon at 55°. Elastically scattered pions appear in channels around 11. Counts in channels around 6 represent positrons and positive muons. Structure of the pulse-height distribution is explained in Sec. 3.

incident beam pulse-height spectrum, calculating the small upward shift due to nuclear recoil and estimating the magnitude of the broadening caused by geometrical effects alone, we could determine the shape of the pulse-height spectrum of the elastically scattered pions and extract the elastic-scattering contribution from any combination of beam components.

The geometrical broadening of the pulse-height spectrum of the scattered beam arises mainly from two causes.

1. The angular divergence of the scattered beam is such that the maximum path length, traversed by the beam in the pulse-height counter, is slightly longer than that traversed during the calibrations. This fact results in an asymmetrical broadening on the high pulse-height side.

2. The difference between the maximum and minimum path lengths within the target is larger for the scattered beam than for the direct beam, on account of the increased angular divergence of the scattered beam.

The half-intensity width of the calibration spectrum was in all cases about 29%. Simple calculations of the geometrical effects led us to the conclusion that their contribution to the width of the elastically scattered pion spectrum should be less than 6% for scattering angles less than 150°. The resultant total width should then be less than 30%. This conclusion is confirmed by the pulse-height spectra obtained in the case of scattering from copper at 40° and from lead at 55°. These are shown in Figs. 4 and 5. The full widths of these spectra are in good agreement with the expected values. Figures 4 and 5 reveal in addition certain tails which are discussed below. Confidence was thus established in the procedure developed for evaluating the number of elastically scattered pions. Typical pulse-height spectra obtained in the case of scattering from carbon are shown in Figs. 6–8. They exhibit a substantial broadening on the high-pulse-height side, which is clearly due to an admixture of events that do not correspond to the elastic scattering of pions. Such events were, therefore, considered in some detail. The broadening of the carbon spectra could be attributed to the presence of positrons, muons, protons, and inelastically scattered pions in the scattered beam.

Positrons can arise from muon decay before or after the analyzing magnet. Positrons of the former kind have the same momentum as the incident pions and their pulse height is much smaller than that of the pions.

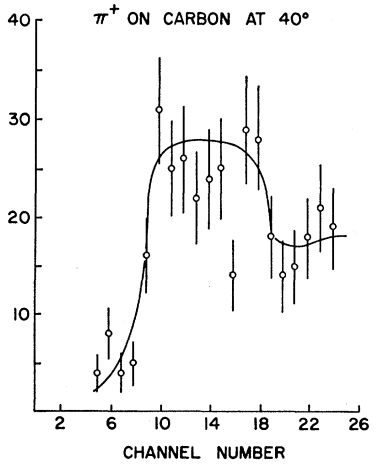

FIG. 6. Pulse-height spectrum for carbon at 40°. Elastically scattered pions appear in channels around 10. Significant contributions from processes other than elastic pion scattering are shown to be responsible for the diffuse nature of the pulse-height spectrum (Sec. 3).

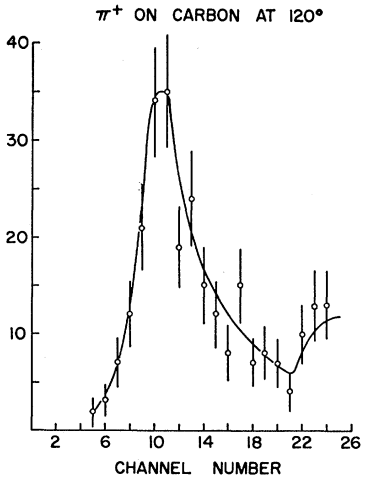

FIG. 8. Pulse-heights pectrum for carbon at 120°. The peak around channel 10 corresponds to elastically scattered pions.

Therefore these positrons are not the cause of the observed broadening of the pulse-height spectrum. The number of positrons of the latter kind, that give a pulse height comparable with or greater than that of the pions, can be estimated and was found to be negligible.

The number of muons arising from direct decay of pions can be estimated from the background and was found to be small. Muons that cannot be attributed to this cause must originate in Coulomb scattering from the target. Coulomb scattering of muons that have the same momentum as the incident pions cannot be the cause of the broadening in the high channels since such muons have slightly less pulse height than the corresponding pions. The alternative processes that give rise to muons in the scattered beam are the following:

(1) Coulomb scattering by the target of a pion through a small angle, followed by decay into a muon;
(2) decay of the pion into a muon, followed by small-angle Coulomb scattering of the muon by the target.

The contributions of both processes were calculated in detail.[17] The contribution of process (1) is two orders of magnitude smaller than that of process (2). The calculations were designed to give the maximum possible contribution of muons. Most of the muons resulting from these processes have β^2 in the neighborhood of 0.28 as opposed to 0.335 for 31.5-Mev pions. Therefore, the pulse height corresponding to these muons was about 20% higher than that of the elastically scattered pions.

Since Coulomb scattering is involved in these processes, the net effect is proportional to Z^2 for a given number of scatterers, where Z is the atomic number of the scattering material. Therefore the effect should be much larger for copper and lead than that in the case of carbon. Hence, significant comparisons can easily be made between these calculations and the observed yields in the case of copper and lead. The comparisons are given in Table I. The agreement between the calculated and the experimentally observed values for copper and lead is worth noting. It leads us to the expectation that similar calculations may be reliable in the case of carbon. However, the observed number of events in the case of carbon is much larger than the calculated number of muons, suggesting the presence of other types of particles having roughly the same pulse height.

TABLE I. Comparison of calculated maximum number of muons with the corresponding number estimated experimentally.

Element	Angle	Maximum number of muons per 10^6 1–2 coincidences: Calculated	Observed
Copper	40°	23.8	20±2.9
Lead	55°	17.0	25±2.9
Carbon	40°	6.6	28±1.9
Carbon	55°	0.8	18.5±1.1

[17] P. P. Kane, Ph.D. thesis submitted to the University of Rochester, 1957 (unpublished).

TABLE II. The ratio, R, of the high-energy proton count to the combined intensity of high-energy protons and inelastically scattered pions.

Angle	R
40°	0.16
55°	0.30
70°	0.40
90°	0.12
120°	0.30
145°	0.30

Protons are produced in stars following the absorption of pions by carbon nuclei. From photographic emulsion work[18–20] such protons are known to have a continuous distribution of kinetic energies, extending up to an energy of about 100 Mev. The thicknesses of the third counter, and of absorbers between the third and the fourth counters, imposed a low-energy cutoff at 17 Mev for observable protons. Introduction of $\frac{1}{32}$-inch copper absorber between counters 3 and 4 in the case of 40° and 55° scattering measurements did not change the 1–2–3–4–$\bar{5}$ counting rate substantially, indicating that most of the observed protons had energies of at least about 30 Mev. Range curves of the scattered beam at 70°, 90°, and 120° showed similarly that rather few low-energy protons were being observed.

We examine next the contribution of high-energy protons. Pulse-height channels around 18 or 19 correspond to an energy dissipation of about 6 Mev in the fourth counter. If high-energy protons appear in these channels, they must have energies above 80 Mev. Unfortunately, pions that have transferred about 10 Mev of excitation energy to the carbon nucleus appear in roughly the same channels. Therefore, additional measurements of 1–2–3–4–$\bar{5}$ counting rates were made with different absorbers between counters 3 and 4, and compared with the zero-absorber pulse-height results. The absorber measurements gave the number of high-energy protons only; the pulse-height data gave the combined intensity of high-energy protons and inelastically scattered pions. Let R be the ratio of the former to the latter. The values of R at different angles are listed in Table II. The error in the determination of R is about 25%. However, it is quite clear that R is less than unity at all angles studied. Therefore, the presence of inelastically scattered pions is established.

There are excited states[16] of carbon at 4.4, 7.6, and 9.6 Mev. The third excited state contributes pions having a pulse height corresponding to channel 18 or 19. We can see a prominent peak around these channels in the case of the carbon pulse-height spectrum at 55°,

[18] Bernardini, Booth, Lederman, and Tinlot, Phys. Rev. 82, 105 (1951).
[19] Bernardini, Booth, and Lederman, Phys. Rev. 82, 1075 (1951).
[20] G. Bernardini and F. Levy, Phys. Rev. 84, 610 (1951).

shown in Fig. 7. Hence, counts in the neighborhood of these channels were attributed mainly to the scattering involving this state. Corrections were made for the possible muon and high-energy proton contaminations discussed above. The possibility of contributions from states around 11 Mev is not ruled out. Our measurements are ambiguous to the extent that such admixtures from higher states are not clearly resolved from the 9.6-Mev state contribution.

Counts in channels 11 to 18, that could not have arisen from protons or elastically scattered pions or muons, were attributed to inelastic pion scattering. As mentioned above, some of these are due to scattering involving the 9.6-Mev state. The rest are contributed by first and second excited state scattering events. During the course of this analysis the number of protons having energies between 25 and 70 Mev was obtained as a by-product.

4. CORRECTIONS AND ERRORS

In order to deduce elastic scattering cross sections, one must apply several corrections to the pulse-height data. The following comments are relevant to the corrections.

(1) Only 91.5% of the incident beam consists of pions.

(2) Counting losses amount to 1% in the case of the measurement of the incident beam.

(3) Efficiency of the 1–3–4 coincidence circuit was determined to be 96.7±2%.

(4) The pion beam traversed roughly 1 g/cm² of the carbon target during each scattering measurement. If we assume a value of 200 mb for the absorption cross section of carbon for pions of this energy, the transmission of the target is seen to be 99%.

(5) Pions decay between counter 2 and the target, and after leaving the target. The first process reduces the pion flux incident on the target. The muon, arising from the second process, might be missed by the scattering counters. The resulting correction for the scattered intensity due to the two cuases is +5%.

(6) Pions interact with absorbers and counter 3. The resulting correction for the scattered intensity is +0.25%.

(7) Muons of the same momentum as the pions are also scattered by the target. They appear at a slightly lower pulse height than the pions but are not clearly resolved from them. The muon contribution to the incident beam was known to be 6.5%. Therefore, the number of scattered muons could be calculated for each angle and subtracted from the number of counts in the appropriate channels to obtain the true elastic scattering contribution.

(8) The finite angular acceptance of the counter telescopes was taken into account at each angle. The correction was quite large in the case of the forward angles but only of the order of 1% at backward angles.

Aside from statistical errors, the most significant uncertainties in the measurement are connected with errors in the determination of (1) efficiency of the 1–3–4 coincidence circuit, (2) orientation of the target, (3) beam purity, and (4) distance between the target and scattering counters. The combined error from these sources is less than 4%. The error arising from impurities in the target was never greater than 7%, even at the smallest angles. The error due to the finite angular acceptance of counters is small at most angles, except in the neighborhood of the minimum in the elastic scattering cross section. Since the inelastic scattering of pions was determined in an indirect manner, the corresponding cross sections are subject to rather large errors which cannot be easily estimated.

5. RESULTS AND DISCUSSION

The final results are given in Table III. The differential cross sections for elastic scattering in the case of the forward angles can be compared with the values to be expected from a pure Coulomb interaction between the pion and the nucleus. We represent the carbon nucleus by means of a uniformly charged sphere and calculate the resulting cross section in the first Born approximation. Since $Ze^2/\hbar v$ is 0.077 for carbon, the approximation is expected to be valid. Here, Ze is the nuclear charge, e and v are the charge and velocity of the pion, and $\hbar$ is Dirac's constant. $f(\theta)$, the amplitude of the pion wave scattered at an angle θ by the nuclear charge, is found to be

$$f(\theta)=-[2\mu Ze^2/\hbar^2K^2]\times 3\times[j_1(KR)/KR], \quad (1)$$

where j_1 is a spherical Bessel function of order 1, K is $2k\sin(\theta/2)$ and k is the pion momentum in wave number units. Thus

$$d\sigma/d\Omega=|f(\theta)|^2=(d\sigma/d\Omega)_c\times 9[j_1(KR)/KR]^2, \quad (2)$$

where $(d\sigma/d\Omega)_c$ is the cross section for point charge. Within the limits of experimental error, the observed elastic scattering cross section of carbon at 40° is equal to the cross section given by Eq. (2). However, the

TABLE III. Cross sections in mb/steradian for various processes involving 31.5-Mev pions. $\sigma_0(\theta)$ is the differential elastic scattering cross section. $\sigma_{12}(\theta)$ is the differential cross section for scattering involving the excitation of the 4.4-Mev and 7.6-Mev states of carbon. $\sigma_3(\theta)$ is the differential cross section for the 9.6-Mev state scattering. $\sigma_p(\theta)$ is the differential cross section for the production of protons from about 25 to 70 Mev.

Element	Laboratory angle	$\sigma_0(\theta)$	$\sigma_{12}(\theta)$	$\sigma_3(\theta)$	$\sigma_p(\theta)$
Carbon	40°	4.77±0.68	0.68±0.65	6.60±0.98	3.0±0.52
	55°	0.72±0.16	0.70±0.25	4.28±0.59	3.0±0.40
	70°	3.79±0.35	1.1 ±0.35	1.3 ±0.29	2.6±0.39
	90°	3.98±0.38	1.0 ±0.3	1.6 ±0.3	2.1±0.33
	105°	6.45±0.58	0.64±0.30	1.0 ±0.24	2.2±0.35
	120°	6.48±0.50	1.2 ±0.40	1.5 ±0.33	2.8±0.40
	145°	7.25±0.63	1.2 ±0.28	2.0 ±0.37	2.3±0.40
Copper	40°	125±14.0			27±5.4
Lead	55°	298±23.0			25±5.0
	70°	18±6.4			24.5±6.5
	90°	41.4±4.1			29±2.9

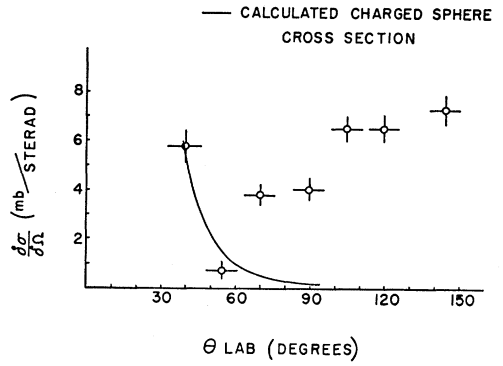

FIG. 9. Angular distribution of the elastic scattering cross section of carbon in the laboratory system for positive pions at 31.5 Mev. The solid curve was computed in the first Born approximation with the use of a charged-sphere model for the nucleus.

observed value at 55° is lower than the computed value (Fig. 9), suggesting destructive interference between the specifically nuclear and the Coulomb scattering amplitudes. This effect was observed previously by Williams *et al.*[21]

The data on elastic pion scattering from carbon at low energies are summarized in Table IV. The variation in the case of the backward elastic scattering cross sections from 31.5 to 40 Mev is small. Further, as the kinetic energy of the pions diminishes, the minimum in the elastic scattering cross section shifts toward smaller angles.

We shall now discuss the results on inelastic scattering. Bernardini and Levy,[20] Byfield *et al.*,[3] and Miller[22] have established the existence of inelastic pion scattering from carbon leading to energy losses greater than 15 Mev. The energy resolution of the three experiments was not good enough to identify inelastic scattering processes involving the first few excited states of carbon. Both the 80-Mev experiment[4] at Columbia and the present experiment show the presence of the latter type of inelastic scattering. In the case of 40-Mev measurements,[5] no attempt was made to establish the existence of inelastic scattering, although it might have been possible to do so. The 80-Mev experiment with negative pions shows a steady increase of inelastic scattering cross sections, for 5-Mev, 10-Mev, and 15-Mev energy loss, with increasing angle of scattering. The present experiment, done at a much lower energy and with positive pions, gives a rather different angular dependence of the cross sections pertaining to different inelastic processes. The combined cross section for inelastic scattering involving both the 4.4-Mev and the 7.6-Mev excited states of carbon suggests an isotropic distribution from 40° to 145° in the laboratory system (Fig. 10). However, a strong forward peaking is noticeable in the angular distribution of the 9.6-Mev state scattering cross section (Fig. 11). In view of the difference in energy and the sign of the pion charge, our results are not necessarily in disagreement with those at 80 Mev.

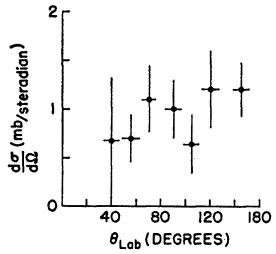

FIG. 10. Angular distribution of the combined cross section for inelastic scattering of 31.5-Mev positive pions involving the excitation of both 4.4-Mev and 7.6-Mev states of carbon.

Experiments on the scattering of protons by carbon in the 10-Mev region[23] give evidence of an angular distribution for scattered protons corresponding to the 4.43-Mev level excitation, which is approximately symmetrical about 90° in the center-of-mass system and which exhibits a minimum at 90°. Deuteron scattering measurements at[24] 15 Mev reveal more complicated angular distributions of inelastically scattered deuterons. A decrease in the inelastic scattering cross sections with increasing angle of scattering is indicated by the electron scattering data.[25] In conclusion, we wish to point out that inelastic scattering processes involving pions, nucleons, deuterons and electrons exhibit angular distributions that are quite characteristic of the nature of the scattered particles.

At 31.5 Mev, the reduced de Broglie wavelength, λ, for pions is 2.4×10^{-13} cm. The radius of the carbon nucleus is less than 2λ. Therefore only S and P states of the incident pion are significantly involved in the scattering process. The pion spin and the spin of the

TABLE IV. Differential cross sections for the elastic scattering of positive pions from carbon at low energies, in mb/steradian.

Angle in laboratory \ Energy	31.5 Mev	40 Mev[a]	60 Mev[b]
40°	5.77±0.68		
45°		2.47±0.82	
55°	0.72±0.16		7±4
60°		2.18±0.16	
70°	3.79±0.35		7±5
90°	3.98±0.38	4.10±0.30	2±2
105°	6.45±0.58		
110°			3±1.6
120°	6.48±0.50	5.36±0.26	
133°			12±5
140°		7.15±0.72	
145°	7.25±0.63		
162°			4±3.5

[a] See reference 5.
[b] See reference 3.

[21] Williams, Rainwater, and Pevsner, Phys. Rev. **101**, 412 (1956).
[22] R. H. Miller, Nuovo cimento **6**, 882 (1957).
[23] M. E. Gove and M. F. Stoddart, Phys. Rev. **86**, 572 (1952); Burcham, Gibson, and Rotblat, Phys. Rev. **92**, 1266 (1953); G. E. Fisher, Phys. Rev. **96**, 704 (1954); H. E. Conzett, Phys. Rev. **105**, 1325 (1957).
[24] J. W. Haffner, Phys. Rev. **103**, 1398 (1956).
[25] J. H. Fregeau, Phys. Rev. **104**, 225 (1956).

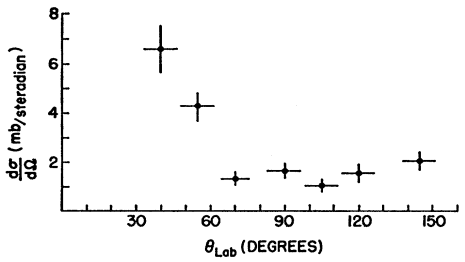

FIG. 11. Angular distribution of the cross section for inelastic scattering of 31.5-Mev positive pions involving the excitation of mainly the 9.6-Mev state of carbon.

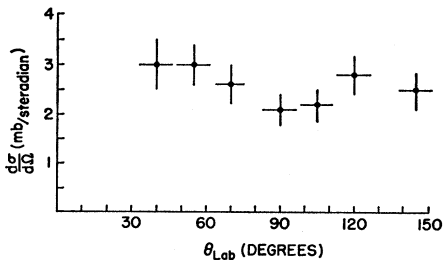

FIG. 12. Angular distribution of the carbon cross section for production of protons in the energy range from 25 to 70 Mev. 31.5-Mev positive pions were incident on carbon.

ground state of C^{12} are zero. The 9.6-Mev state of carbon plays a dominant role in the scattering of positive pions. Hence its spin is unlikely to be larger than two units. This conclusion is in agreement with a suggestion of Morinaga[26] and with a prediction of Glassgold and Galonsky.[27] The latter authors conclude on the basis of the α-particle model that the 9.6-Mev state is 1^- or 2^+. On the assumption that the 9.6-Mev state belongs to the same configuration as the ground state, Pal and Nagarajan[28] deduce the total angular momentum of the 9.6-Mev state to be 2 units, although they have some difficulty in fitting the intermediate-coupling parameter to the energy values of the excited states of carbon. Using a (d,n) reaction, Graue[29] makes an assignment of 1^- to the 9.6-Mev state. This result is in contradiction with the more recent one of Fregeau, obtained by means of electron scattering experiments. The latter suggests the assignment 0^+ or 2^+. Our conclusion is not in conflict with any of the foregoing assignments.

The high-energy protons, produced in interactions of positive pions with carbon nuclei, exhibit an isotropic angular distribution within the experimental uncertainties (Fig. 12). This result is in agreement with that of Byfield *et al.*[3] obtained at 60 Mev.

In conclusion, it may be said that considerably better energy resolution in pion scattering experiments would be very helpful in the analysis of the complex processes that take place.

6. ACKNOWLEDGMENTS

It is a pleasure to thank Dr. E. M. Hafner for many stimulating discussions and constant advice, Dr. M. C. Camac and Dr. Bruce Johnson for work on the pion beam extraction and electronics, and Mr. E. Nordberg for able assistance during the cyclotron runs.

[26] H. Morinaga, Phys. Rev. **101**, 254 (1956).
[27] A. E. Glassgold and A. Galonsky, Phys. Rev. **103**, 701 (1956).
[28] M. K. Pal and M. A. Nagarajan, Phys. Rev. **108**, 1577 (1957).
[29] A. Graue, Phil. Mag. **45**, 1205 (1954).